Gene 646 (2018) 143–152

Contents lists available at ScienceDirect

Gene

journal homepage: www.elsevier.com/locate/gene

Research paper

Molecular cloning and characterization of *APOBEC3* family in tree shrew

Meng-Ting Luo[a,b], Yu Fan[a,b], Dan Mu[a,b], Yong-Gang Yao[a,b,c], Yong-Tang Zheng[a,b,c,d,*]

[a] Key Laboratory of Animal Models and Human Disease Mechanisms of the Chinese Academy of Sciences/Key Laboratory of Bioactive Peptides of Yunnan Province, Kunming Institute of Zoology, Chinese Academy of Sciences, Kunming, Yunnan 650223, China
[b] Kunming College of Life Science, University of Chinese Academy of Sciences, Kunming 650204, Yunnan, China
[c] Kunming Primate Research Center of the Chinese Academy of Sciences, Kunming Institute of Zoology, Chinese Academy of Sciences, Kunming 650223, China
[d] KIZ-SU Joint Laboratory of Animal Models and Drug Development, College of Pharmaceutical Sciences, Soochow University, Suzhou, Jiangsu 215006, China.

ARTICLE INFO

Keywords:
Tree shrew
Innate immunity
APOBEC3
Restriction factor
Cytidine deaminase

ABSTRACT

The APOBEC3 family is a series antiviral factors that inhibit the replication of many viruses, such as HIV-1 and HBV. Tree shrews (*Tupaia belangeri*) possess great potential as an animal model for human diseases and therapeutic responses. However, the APOBEC3 family is unknown in tree shrews. Recent work has showed the presence of the APOBEC3 family in tree shrews. In this work, the cDNA sequences of five *APOBEC3* members were identified in tree shrews, namely, *tsAPOBEC3A*, *-3C*, *-3F*, *-3G* and *-3H*. The results showed that their sequences encoded a zinc (*Z*)-coordinating-domain as a characteristic of APOBEC3 proteins. Phylogenetic analysis revealed that the tree shrew *APOBEC3* (*tsAPOBEC3*) *genes* have occurred independently and that they are clustered with other mammalian *APOBEC3* members. Transcript expression analysis indicated that *tsAPOBEC3 genes* are constitutively expressed, and high in immune-related tissues. *tsAPOBEC3 gene* expression was up-regulated in hepatocytes and PBMCs by IFN-α stimulation. Finally, tsAPOBEC3 proteins could edit both sides of DNA by inserting G → A and C → T hypermutations. Overall, the results suggest that the tsAPOBEC3 family could play a key role in defense immunity through distinct editing mechanisms. Our results provided insights into the genetic basis for the development of a tree shrew model for studying viral infection. Future studies will focus on deepening our understanding on the antiviral functions of these editing enzymes in tree shrew.

1. Introduction

The development of the innate immunity first-line barrier to pathogens has been driven by interactions between host factors and viruses. As a parasite, most viruses depend on host factors to complete their replication cycles due to their limited genome size. In contrast, the host has evolved restriction factors to intervene against the replication of various viruses, including interferon-stimulated genes (ISGs) (Zheng et al., 2012). Several ISGs which could insert hypermutation in many different viruses belong to the cytidine deaminase family (Chen and MacCarthy, 2017; Stavrou et al., 2015). These enzymes include the activation-induced cytidine deaminase (AID)/apolipoprotein B mRNA-editing enzyme catalytic polypeptide proteins (APOBEC) family, which promotes specific RNA/DNA editing by deaminases (Rogozin et al., 2005). In humans, the *APOBEC3* family is comprised of seven members, including *APOBEC3A*, *-3B*, *-3C*, *-3DE*, *-3F*, *-3G* and *-3H* (Zheng et al., 2012), which confer restrictions on major viruses such as human immunodeficiency virus 1 (HIV-1) (Bishop et al., 2008; Dang et al., 2008; Mohanram et al., 2013; Nowarski et al., 2014; Sakurai et al., 2015), hepatitis B virus (HBV) (Henry et al., 2009; Janahi and McGarvey, 2013; Nguyen et al., 2007; Seppen, 2004), herpesviruses (Nakaya et al., 2016), papillomaviruses (Wang et al., 2014), and trans-elements, including Alu and LINE-1 (Koyama et al., 2013). The APOBEC3 family preferentially deaminates single-stranded DNA (ssDNA), resulting in mixed premature termination codons in viral genome DNA due to G → A hypermutations in the process of virus post-replication process (Vieira and Soares, 2013; Zheng et al., 2012).

Tree shrews (*Tupaia belangeri*) possess great potential as an animal model for human diseases and therapeutic responses and are distributed in South Asia and Southwest and South China (Cao et al., 2003; Fan

Abbreviations: 3DPCR, differential DNA denaturation PCR; A, adenosine; AID, activation-induced cytidine deaminase; APOBEC, apolipoprotein B mRNA-editing enzyme catalytic polypeptide proteins; APOBEC3, apolipoprotein B mRNA-editing enzyme catalytic polypeptide-like 3 proteins; Btau, *Bos taurus*; C, cytidine; CDS, coding sequences; Ecab, *Equus caballus*; FBS, fetal bovine serum; Fcat, *Felis catus*; G, guanosine; Ggor, *Gorilla gorilla*; HBV, hepatitis B virus; HCV, hepatitis C virus; HIV-1, human immunodeficiency virus 1; Hsap, *Homo sapiens*; IFN, interferon; IL-2, interleukin-2; ISG, interferon-stimulated gene; MAVS, mitochondrial antiviral signaling; MHC, major histocompatibility complex; Mmul, *Macaca mulatta*; Mmus, *Mus musculus*; Nleu, *Nomascus leucogenys*; ORF, open reading frame; Pabe, *Pongo abelii*; PCR, polymerase chain reaction; PFA, paraformaldehyde; Ptro, *Pan paniscus*; RACE, rapid amplicate of cDNA end; Rnor, *Rattus norvegicus*; RT-PCR, real-time PCR; SIV, simian immunodeficiency virus; T, thymidine; Tbel, *Tupaia belangeri*; TRIM, tripartite motif

* Corresponding author at: Kunming Institute of Zoology, CAS, China.
E-mail address: zhengyt@mail.kiz.ac.cn (Y.-T. Zheng).

https://doi.org/10.1016/j.gene.2017.12.060
Received 9 September 2017; Received in revised form 27 December 2017; Accepted 28 December 2017
Available online 30 December 2017
0378-1119/

et al., 2013). Tree shrews are susceptible to many human viruses and bacterial infections (Li et al., 2012; Xu et al., 2013). Many attempts have been made to employ tree shrews as animal models and replace nonhuman primates when studying HBV (Kayesh et al., 2017; Walter et al., 1996; Xiao et al., 2017) and hepatitis C virus (HCV) (Zhao et al., 2002), influenza virus (Yang et al., 2013), herpes simplex virus (Darai et al., 1978; Li et al., 2016), Coxsackie virus A16 (Li et al., 2014), dengue infection (Kayesh et al., 2017), social stress and depression (Fuchs, 2005), brain development and aging (Wei et al., 2017), basal cell carcinoma (Jiang et al., 2017), embryonic development and transplantation (Yan et al., 2016), due to its unique characteristics, including its small body size, short reproductive cycle and life span, low cost of maintenance, and close relationship to primates (Fan et al., 2013; Novacek, 1992; Xu et al., 2013). In previous work, there are many descriptions of tree shrew models for human disease research (Zheng et al., 2014). Indeed, using the tree shrew as an experimental animal is less controversial than primates and has fewer ethical concerns (Yao, 2017).

A previous study showed that HBV genome editing profiles containing G to A hypermutations (Renard et al., 2010) in HBV-infected tree shrew primary liver cultures are similar to those observed in humans. This revealed that there are APOBEC3 factors in tree shrews. However, there is a quite difference between the quantity of *APOBEC3* family members in different species (LaRue et al., 2009; Munk et al., 2012). Due to these features, APOBEC3 proteins may have distinct capabilities in different species. APOBEC3 proteins provide a barrier for the cross-species transmission of viruses, such as simian immunodeficiency virus (SIV). APOBEC3s protect chimpanzees against lentiviruses from monkeys, as chimpanzee APOBEC3G could not be antagonized by SIVwrc or other SIVs (Etienne et al., 2015). In the function of editing, murine APOBEC1 but not human APOBEC1 could deaminate cytidine residues in murine leukemia virus genomic RNA (Petit et al., 2009). Identification of the APOBEC3 family in tree shrews will help to answer why tree shrews can be infected by many viruses and will contribute to understanding the immune system of the tree shrew. In this study, we characterized *APOBEC3* orthologs in tree shrews for the first time and determined the structure of tsAPOBEC3 functional domains. We also constructed a phylogenetic tree and analyzed the evolutionary and selective pressures on *tsAPOBEC3 genes*. Furthermore, *tsAPOBEC3 genes* expression patterns in different tissues or when stimulated by IFN-α and its editing ability were investigated. Our study indicated the conservation and specificity of *APOBEC3 genes* between tree shrews and other mammals.

2. Materials and methods

2.1. Collection of tree shrew tissues and determination of tsAPOBEC3 sequences

Tree shrews were raised at the experimental core facility at Kunming Institute of Zoology, Chinese Academy of Sciences. Brain, heart, liver, lung, spleen, colon, and other tissue samples were isolated from three healthy male adult tree shrews, immediately frozen in liquid nitrogen and then stored at − 80 °C. All experimental procedures were performed according to the guidelines approved by the Ethics Committee of the Kunming Institute of Zoology (approval number: SWYX-2013023).

Total RNA was extracted from tree shrew spleen tissue by using TRIzol (Invitrogen). The SMARTer™ RACE cDNA Amplification Kit (RACE Kit, Clontech) was used to obtain the 5′- and 3′- ends of the full length *tsAPOBEC3* transcripts based on other mammalian APOBEC3 sequences (Table S1). We used Open Reading Frame Finder (ORF Finder, http://www.ncbi.nlm.nih.gov/gorf/orfig.cgi) to define the full-length coding sequences (CDS).

2.2. Phylogenetic analysis

The CDSs were aligned with the guidance of aligned protein sequences with MUSCLE 3.7 (http://www.ebi.ac.uk/Tools/msa/muscle/), which was concatenated the sequences into one super gene for each species. Then, RAxML 8.0.0 (Stamatakis, 2014) (http://sco.h-its.org/exelixis/software.html) was applied to the sequence sets to build a phylogenetic tree using the BLOSUM62 + gamma model for protein sequences. We employed 1000 rapid bootstrap replicates to assess the branch reliability in RAxML 8.0.0. Information on the sequences used is listed in Table S1.

2.3. Divergence time estimation

PAML4.7 (Yang, 2007) MCMCtree was used to determine the split times with approximate likelihood calculations. The PAML baseml was first taken to estimate the per site substitution rate for the nucleotide data set. Then, we estimated the gradient (g) vector and Hessian (H) matrix, which describe the shape of the log-likelihood surface around maximum likelihood estimates (MLE) of branch lengths. The “Correlated molecular clock” and “REV” substitution models were used for the estimation. The gamma prior to the overall substitution rate was described by the shape and scale parameters, which were set as 1 and 1.8, respectively, and were calculated according to the substitution rate per time unit. The alpha parameter for the gamma rates at the sites was set as the value computed by baseml in the first step. After a 1 million iterations burn-in, the MCMC process in PAML MCMCtree was run to sample 10 thousand times, with the sample frequency set to 1000. The “finetune” parameters were set as “0.08438, 0.20815, 0.03932, 0.10000, and 0.30000”. Other parameters were set to default.

2.4. Quantitative real-time PCR

The total RNA was prepared for cDNA synthesis using the PrimeScript RT reagent Kit with gDNA Eraser (TaKaRa) from three healthy male adult tree shrews' tissues. The cDNA was used for real-time PCR (RT-PCR) to detect *tsAPOBEC3 mRNA* expression, using the qtsA3s primers with normalization to the *PRL13A gene* (Table S2).

2.5. Western blot

293 T cells were transiently transfected with the pNL4-3 and tsAPOBEC3 plasmids. Forty-eight hours after transfection, the cells were lysed for 30 min on ice with lysing agent (Beyotime, P0013) and PMSF. The cell lysates were centrifuged at 13,000*g* for 10 min at 4 °C and the supernatants were transferred into a clean 1.5 mL Eppendorf tube and stored at − 80 °C.

The prepared proteins were separated by sodium dodecyl sulfate polyacrylamide gel electrophoresis (SDS-PAGE) and then transferred onto polyvinylidene fluoride (PVDF) membranes (Millipore). After blocking with non-fat milk, the blots were probed with mouse HA antibody (Sigma) or mouse anti-hAPOBEC3G antibody (ImmunoDiagnostics) to detect tsAPOBEC3-HA or tsAPOBEC3 proteins. Anti-β-actin mouse monoclonal (CWBIO) or anti-β-Tubulin rabbit polyclonal (Epitomics) antibodies were used to detect actin or tubulin controls, respectively. Then, the membranes were incubated with goat anti-mouse or anti-rabbit IgG secondary antibodies. Afterwards, the blots were illuminated with chemiluminescent detection reagents (Millipore) via X-ray film. Information on the antibodies used is listed in Table S3.

2.6. Plasmids, cell cultures and transfection

The pcDNA3.1-tsAPOBEC3A/C/F/G/H-HA plasmids were generated by inserting the tsAPOBEC3 cDNA into the EcoR I or Hind III and *Xba* I site of pcDNA3.1(+) (Invitrogen), which fused an HA epitope tag to its

carboxyl terminus. The Δvif-pNL4-3 plasmid was a generous gift from Dr. Guangxia Gao (Institute of Biophysics, CAS).

HepG2, 293 T and Tzm-bl cells were cultured in Dulbecco's modified Eagles' medium (DMEM) with 10% Fetal Bovine Serum (FBS). Lipofectamine 2000 (Invitrogen) was used to transiently transfect the plasmids into cells according to the manufacturer's protocol.

2.7. Immunofluorescence microscopy

Forty-eight hours post-transfection, HepG2 cells climbing to the carry sheet glass, were washed once with PBS and then fixed with 4% paraformaldehyde (PFA) (Sigma) for 15 min at room temperature. The cells were washed three times for 5 min with PBS and then permeabilized with 0.1% Triton X-100 (Sigma). Slides were washed three times for 5 min with PBS, and then the cells were blocked for 30 min with 2% BSA (Sigma) at room temperature. The fixed cells were incubated with anti-HA primary antibody (Sigma) for 2 h at room temperature. After washing with PBS three times, the cells were incubated at room temperature in the dark for 1 h with rhodamine-labeled secondary antibody (cwbiotech). After extensive washing, the slides were incubated with DAPI (1 μg/ml; Beyotime) for 5 min. Then, the cells were washed again with PBS and the slides were mounted on glass slides with Antifade Mounting Medium (Beyotime). Images from the slides were captured using an Olympus FV10 confocal microscope (Olympus, Germany). The antibody information is recorded in Table S3.

2.8. Isolation and cultivation of primary tree shrew hepatocytes or PBMCs and IFN-α stimulation

We used a two-step collagenase perfusion method, with some modifications, to isolate primary tree shrew hepatocytes (Kock et al., 2003). Briefly, the liver was perfused via the portal vein with Hanks' solution containing 5 mmol/L EGTA (Sangon Biotech) for 5 min, and then with Hanks' solution containing 5 mmol/L $CaCl_2$ and 0.5 mg/ml collagenase IV (Sigma) for 10 min at 37 °C. The cells were washed twice with PBS, seeded onto 6-well plates, and then maintained in 2 ml DMEM with 10% fetal bovine serum (FBS), 100 units/ml penicillin (Sigma), 100 μg/ml streptomycin (Sigma), 0.15% BSA (Sigma), 0.1 μM dexamethasone (Suicheng Pharm), and 10 μg/ml insulin (Wanbang BioPharm). Blood from tree shrew was collected via venipuncture. The PBMCs were purified by Ficoll density centrifugation. The purified PBMCs were grown in RPMI 1640 medium containing 10% FBS and interleukin-2 (IL-2, 50 U/ml).

After the cells rested overnight, they were cultured in the presence or absence of 1000 U/ml recombinant human IFN-α2β. Samples were taken at the start of culture (time point 0 h) and after 12 h of culture. Total RNA was isolated and reverse transcribed, and then relative mRNA induction was determined by quantitative PCR with normalization to *RPL13A mRNA*.

2.9. Hypermutation of viral DNA in vitro

The Δvif-pNL4–3 HIV-1 plasmid was transiently co-transfected with the APOBEC3 expression plasmid or pcDNA3.1 (+) control plasmid in a 5:1 ratio into 293 T cells as described above. After 48 h, the viral supernatant was collected to infect TZM-bl cells. Forty-eight hours post-infection, the infected TZM-bl cells were washed with PBS and total cellular DNA was extracted using a DNeasy DNA isolation kit (Qiagen). The extracted DNA was used in the hypermutation test. The two-step PCR/differential DNA denaturation PCR (3DPCR) approach has been previously described (Renard et al., 2010). The primers for the nested PCR were as follows: (1) 5′-CAG AGC CAA CAG CCC CRC CA-3′ (PRO-1, first round, forward), (2) 5′-TGG AAA TGT GGR AAR GAA GGA C-3′ (AW26, first round, reverse); (3) 5′-CTG TAY TTC TGC TAY TAA GTC TTT TGA TGG G-3′ (RT21, first round, forward), and (4) 5′-CTG CCA RTT CTA RYT CTG CTT C-3′ (RT20, first round, reverse).

The following conditions were used for the first round of PCR: (1) 94 °C for 3 min; (2) followed by 94 °C for 30 s, 50 °C for 30 s and 72 °C for 1 min for 30 cycles, and (3) a final extension at 72 °C of 10 min. The first-round PCR products were diluted 20 times and used as a template for the second round of PCR. 3DPCR was performed with the following conditions: (1) 84 °C for 5 min; (2) followed by 84 °C for 30 s, 50 °C for 30 s and 72 °C for 1 min for 35 cycles; and (3) finally 10 min at 72 °C. PCR products were purified from agarose gels and ligated into the pMD-19 T cloning vector. After the transformation of DH5α cells, we selected 13–18 clones for sequencing. Hypermutation analysis was performed using the HYPERMUT program (http://hiv-web.lanl.gov/HYPERMUT/hypermut.html).

2.10. Statistical test

The data are presented as the mean ± standard deviation (SD). Differences between groups were analyzed using the Student's *t*-test. A significant difference was scored as * $p < 0.05$, ** $p < 0.01$ and *** $p < 0.001$.

3. Results

3.1. Identification, cDNA cloning and sequence analyses of five APOBEC3 members in the Chinese tree shrew (Tupaia belangeri)

Based on the reported mammalin *APOBEC3* gene sequences (LaRue et al., 2009; Munk et al., 2012) and the tree shrew genome sequence (Fan et al., 2013; Fan et al., 2014), partial cDNA sequences for *tsAPOBEC3 genes* were identified. We amplified cDNA from total RNA extracted from tree shrew spleen and identified five full-length *tsAPOBEC3 genes* via 5′−/3′- RACE as described previously (Xu et al., 2015).

The *tsAPOBEC3* ORF regions were identified using ORF finder. As shown in Fig. 1A, Fig. 1B and Table 1, the *tsAPOBEC3 genes* consisted of sequences containing 2–6 exons spanning 465–1098 bp cDNA, 155–366 amino acids. Each *tsAPOBEC3 gene* has a single- or a double-zinc (*Z*)-coordinating-domain similar to humans (Fig. 1B), which is identified by one histidine, one glutamate, and two cysteines organized as $HxEx_{23-28}PCx_{2-4}C$ (x can be any amino acids); this is a characteristic of APOBEC3 protein sequence (LaRue et al., 2009). Only the tsAPOBEC3G N-terminal Z domain is slightly different from the others (Fig. 1B). Although there is a quite a difference in the number of *APOBEC3* family members in different species, the genes were arranged in a reverse sequential order from *CBX6* to *CBX7* (Fig. 1C). Each *Z*-domain clearly belongs to one of three distinct phylogenetic clusters, which were originally termed Z1, Z2, and Z3 for their key identifying residues (LaRue et al., 2009). According to the *APOBEC3* family naming rule in non-human primates, *APOBEC3 genes* from tree shrew were renamed *A3Z1a, A3Z2a-Z2b, A3Z2c-Z1b, A3Z2d-Z2e* and *A3Z3*, corresponding to *APOBEC3A*, *-3C*, *-3G*, *-3F*, and *-3H*, respectively (Fig. 1C and Table 1).

Although these simple rules enable the assignment of the initial Z-domain, it should be noted that each Z-domain is different from the other. The multiple sequence alignment revealed the several conserved motifs and amino acids in the APOBEC3 family Z-domain. The multiple alignment was performed to assess the conservation between the APOBEC3 family Z-domain between tree shrew and other mammals (Fig. 2). This analysis showed a high identity among the tsAPOBEC3 Z-domains, demonstrating its homologous with other mammalian *APOBEC3 genes*. Additionally, *tsAPOBEC3 genes* could be named according to the amino acids identified in the Z-domain (LaRue et al., 2009).

3.2. APOBEC3 family in tree shrew evolved independently and underwent selected stresses

The phylogenetic relationships between the *tsAPOBEC3* sequences

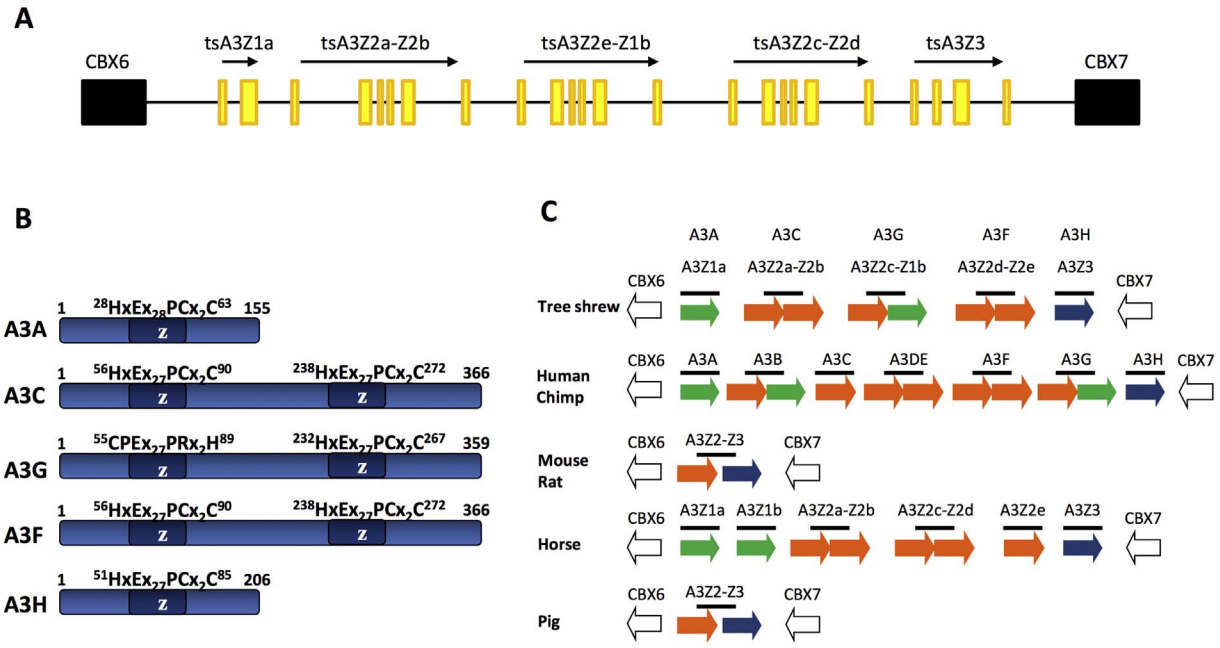

Fig. 1. Schematic representation of the tree shrew APOBEC3 domain architecture. The predicted proteins included a totally conserved structural organization. Similar to proteins in other mammalian species, tree shrew APOBEC3 proteins included *Z*-domain motifs such as $HxEx_{23\text{-}28}PCx_2C$ (x can be any amino acid), except for the A3G N-terminal site. (A) The *APOBEC3* family exons in Chinese tree shrews are marked by yellow boxes. (B) The tsAPOBEC3 members Z-domains motifs are shown in schematic structures. (C) Schematic profile of the *APOBEC3* repertoires from seven mammalian species. Z1, Z2, and Z3 domains are shown in green, orange and blue, respectively. For all the indicated species, *CBX6* is located upstream and *CBX7* downstream of the *APOBEC3* locus. (For interpretation of the references to colour in this figure legend, the reader is referred to the web version of this article.)

Table 1
The characteristics of tree shrew (*Tupaia belangeri*) *APOBEC3* coding sequences (CDS).

APOBEC3	CDS length (bp)	Length (amino acids)	Domains identified	Z domain position (amino acids)	GenBank accession number
tsA3A	465	155	Z1a	28–63	KU053484
tsA3C	1098	366	Z2a	56–90	KU053485
			Z2b	238–272	
tsA3G	1077	359	Z2c	55–89	KU053487
			Z1b	232–267	
tsA3F	1098	366	Z2d	56–90	KU053486
			Z2e	238–272	
tsA3H	618	206	Z3	51–85	KU053488

were analyzed. In Fig. 3A, the results from the evolutionary analysis deduced that ts*APOBEC3* sequences were clustered in the same branch with other animals. However, ts*APOBEC3A*, *-3C*, *-3G* and *-3F* (*A3Z1a*, *A3Z2a-Z2b*, *A3Z2c-Z1b*, and *A3Z2d-Z2e*) were clustered in one branch. This illustrated that they were evolved independently. Moreover, the A3Z motif evolutionary analysis showed that the two tsA3Z1 motifs and five tsA3Z2 motifs also evolved independently (Fig. 3B). Simultaneously, divergence time analysis showed that the two tsA3Z1 and five tsA3Z2 motifs diverged nearly before 32.2 million years ago (Fig. 3C).

Evidence for the positive selection was analyzed using CODEML from the PAML4.7 package (Yang, 2007). The alignments for the *A3Z1*, *A3Z2* and *A3Z3* genes were analyzed separately from the whole sequence set. The positive selection analysis results showed that only A3Z2 has a positively selected site (Table 2).

3.3. *tsAPOBEC3 expression pattern in different tissues*

We used qPCR to detect the tissue-specific expression patterns of *tsAPOBEC3* family genes from tissue-specific cDNA samples from three male tree shrews. Simultaneously, we also examined the tsAPOBEC3 proteins by western blot. The data revealed that the *tsAPOBEC3* transcripts and proteins have significantly higher expression levels in the spleen (the largest secondary lymphoid organ), which comprises the most important immune defense tissues (Fig. 4A and B). Additionally, *tsAPOBEC3* mRNA levels were also highly expressed in the colon and blood (Fig. 4A). tsAPOBEC3 proteins were detected by anti-hAPOBEC3G mouse antibodies and displayed high levels in the spleen, colon and ileum (Fig. 4B). Confocal microscopy showed that most of the tsAPOBEC3 proteins were localized in the cytoplasm, while tsAPOBEC3A and -3C were localized in the nucleus (Fig. 3C), from where the proteins could gain access to the DNA in the nucleus.

3.4. *APOBEC3 expression was induced by IFN-α2β stimulation in tree shrew primary hepatocytes and PBMCs*

As intrinsic viral resistant factors, APOBEC3 proteins have the capacity to inhibit viruses at the onset of host infection or exposure (Zheng et al., 2012). Therefore, it is reasonable to contend that the expression of these proteins might be under the regulation of cytokines that play a role in early responses to virus infection, such as type I interferon. Previous studies had shown a possible effect for IFN-α on human *APOBEC3G* expression (Koning et al., 2009). Additionally, *APOBEC3 genes* have been previously identified as ISGs. As hepatocytes are the major target cells for HBV replication and CD4 + T cells among PBMCs for HIV-1 during natural infection in humans, we assessed the induction of *tsAPOBEC3* gene expression in tree shrew primary hepatocytes and PBMCs. Thus, cDNAs from tree shrew primary hepatocytes and PBMCs were obtained and *tsAPOBEC3* gene expression was assessed by RT-qPCR 12 h after IFN-α2β stimulation. The results showed that *tsAPOBEC3 genes* had a differential overexpression in the hepatocytes and PBMCs. First, all five *tsAPOBEC3 genes* showed relative expression patterns in the hepatocytes and PBMCs in response to IFN-α2β. A highlighted overexpression in *tsAPOBEC3 genes* was observed in the analyzed hepatocytes, except for *tsAPOBEC3A* (Fig. 5A). The expression of *tsAPOBEC3F* showed a nearly 30-fold change compared to cells treated with PBS at the evaluated time point in hepatocytes. The expression of *tsAPOBEC3C* showed a nearly 20-fold change and

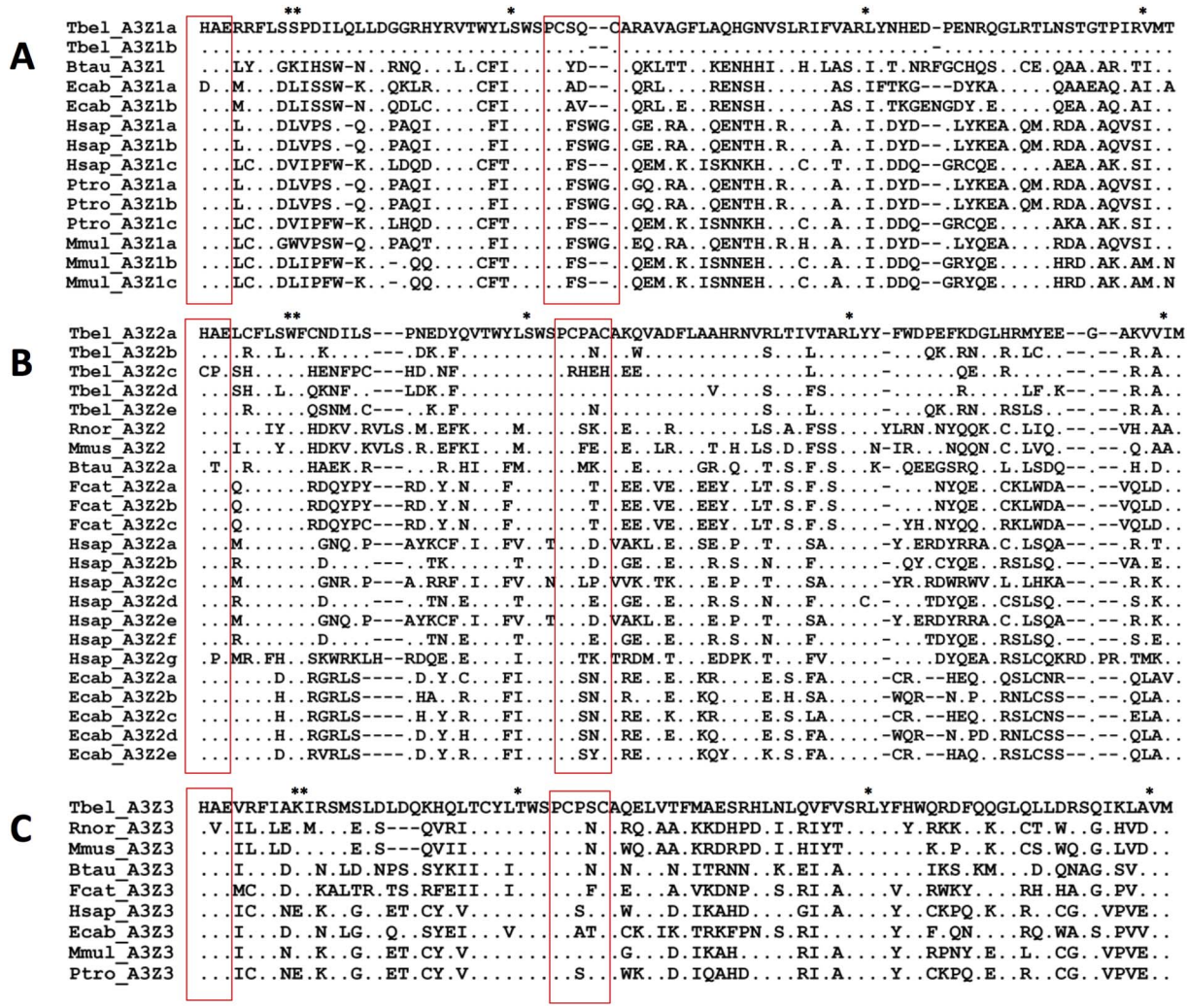

Fig. 2. Multiple sequence alignment of the APOBEC3 Z domain. Sequences from tree shrews were aligned with other mammalian Z domains, (A) Z1 (B) Z2 and (C) Z3. The key functional editing domain is boxed. The naming rule amino acids are marked by asterisks.

tsAPOBEC3G showed a nearly 10-fold change. However, only slight *tsAPOBEC3A* overexpression was observed in the analyzed hepatocytes, whereas no significant differences were found in PBMCs. The expression of all the *tsAPOBEC3 genes* showed < 5-fold changes in PBMCs (Fig. 5B). The results were similar to those in human cells (Tanaka et al., 2006; Wang et al., 2008).

3.5. APOBEC3 in tree shrew could edit both side of DNA through deaminase-dependent mechanisms

To specifically address the role of tsAPOBEC3 proteins in DNA editing, we aimed to confirm the impact of tsAPOBEC3 proteins to promote the G → A hypermutation on integrated HIV-1 DNA with hAPOBEC3G as a positive control and no APOBEC3 as a negative control. Standard PCR was used for the first round and 3DPCR for the second round (Renard et al., 2010). All tsAPOBEC3 proteins could hyperedit HIV-1 DNA based on the 3D-PCR products (Fig. 6A). The 3DPCR products recovered at the restrictive temperature of 84 °C were cloned, and 13 to 18 clones were sequenced. Cytidine deaminase activity resulted C → U hypermutants; therefore, the C → U hypermutant in the cDNA minus-strand showed a G → A hypermutant in the plus-strand DNA and the C → U hypermutant in the plus-strand DNA showed a C → T hypermutant in the plus-strand DNA during the HIV-1 reverse transcription procession. Mutation matrices for the hAPOBEC3G and tsAPOBEC3s hypermutants were compared to the HIV-1 NL4-3 viral plus strand sequences. As seen in Fig. 6A, molecular cloning and sequencing showed that the tsAPOBEC3 hypermutants contained G → A and C → T transitions, while hAPOBEC3G hypermutants mainly contained G → A transitions in the plus strand DNA. This indicated that all tsAPOBEC3 enzymes could extensively deaminate the minus and plus strands. The 5′-dinucleotide context editing preference showed a bias for TpC and GpC by tsAPOBEC3 proteins in the minus strand (Fig. 6B). However, C → T transitions showed a penchant for TpC by tsAPOBEC3s in the plus strand (Fig. 6C) The positive control observed in Fig. 6B showed that hAPOBEC3G prefers to mutate the minus strand 5′-CC → CU and promote a plus strand 5′-GG → AG mutation as was previously mentioned (Zheng et al., 2012) but is unable to promote C → T transitions. Analysis of the tsAPOBEC3s GC → AT transitions is reminiscent of APOBEC3s editing in humans. However, the dinucleotide context for the G → A and C → T transitions by tsAPOBEC3 proteins revealed a penchant for TpC, demonstrating a special feature in tsAPOBEC3s editing.

4. Discussion

APOBEC3 proteins are important enzymes for restricting viral replication. In hosts, retroviral genomes undergo cytidine deamination to introduce multiple mutations by APOBEC3 proteins due to the highly variable nature of APOBEC3 (Munk et al., 2012). The identification of APOBEC3 provides new insights into manipulating the innate immune

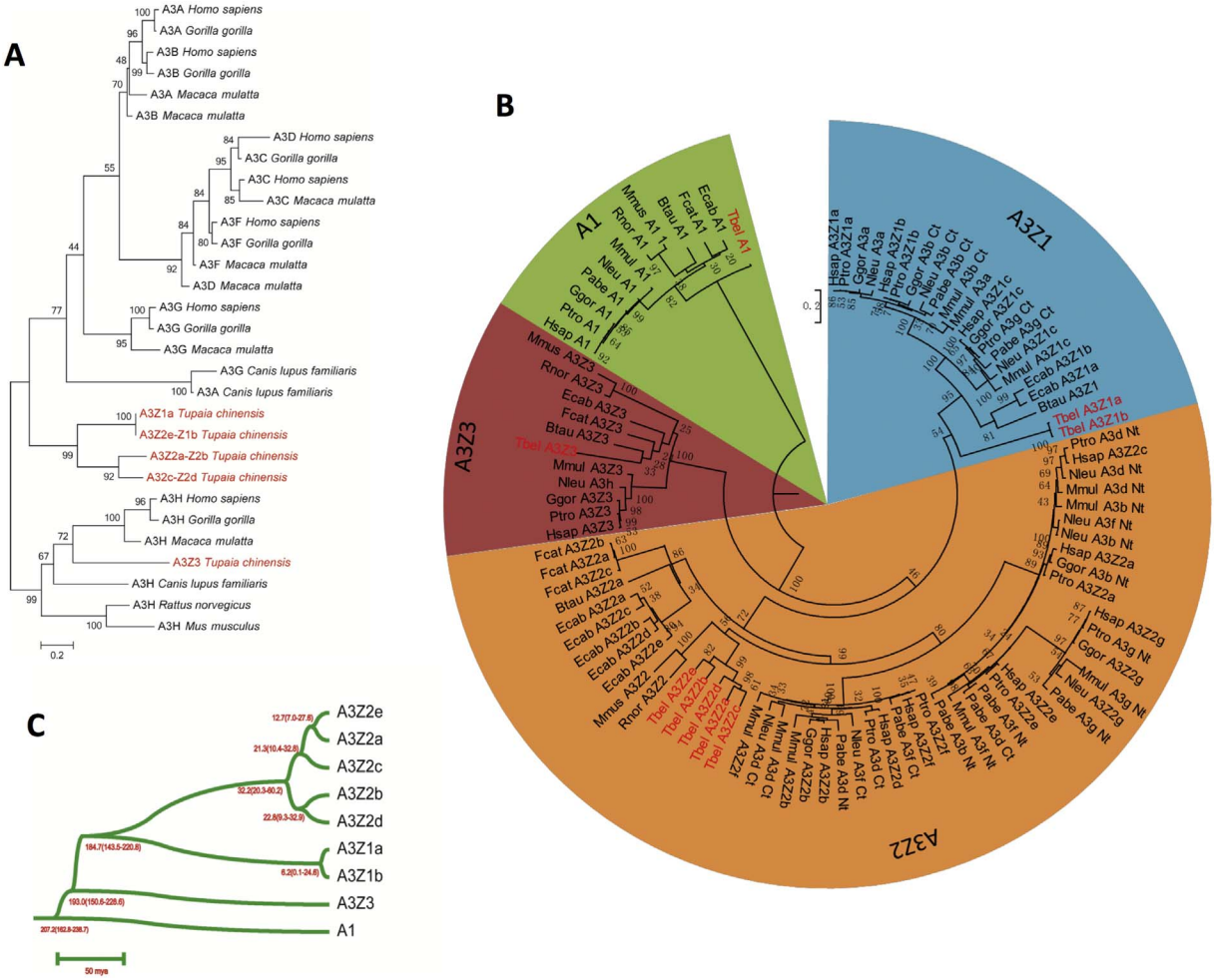

Fig. 3. Phylogenetic tree of tree shrew APOBEC3 family. (A) Evolution of the *tsAPOBEC3* family, including *A3Z1a, A3Z2a-Z2b, A3Z2c-Z2d,* and *A3Z2e-Z1b* (*tsAPOBEC3A*, *-3C*, *-3G*, and *-3F*), in tree shrews evolved independently of others. (B) The Z domains in the *tsAPOBEC3* family, including *A3Z1a* and *A3Z1b, A3Z2a-Z2b, A3Z2c-Z2d* and *A3Z2e* from tree shrews evolved independently of others respectively. (C) Divergence time of the *APOBEC3* family in tree shrews. The *tsAPOBEC3* family blossomed 32.2 mya (million year ago), which occurred after tree shrew speciation (Roberts et al., 2011). The abbreviation of repertoire species and sequence sets are shown in Table S1.

Table 2
The tree shrew (*Tupaia belangeri*) APOBEC3 positive selection analysis.

Foreground	p-Value	Positively selected sites (BEB analysis)	Parameters
tsA3Z1a	0.9988716	NA	p0 = 0.35687 p1 = 0.44966 p2a = 0.08561 p2b = 0.10787 w0 = 0.10491 w1 = 1.00000 w2 = 1.05019
tsA3Z1b	0.9984042	NA	p0 = 0.37911 p1 = 0.47769 p2a = 0.06336 p2b = 0.07984 w0 = 0.10491 w1 = 1.00000 w2 = 1.31539
tsA3Z1	0.1947566	NA	p0 = 0.40253 p1 = 0.47388 p2a = 0.05676 p2b = 0.06683 w0 = 0.09965 w1 = 1.00000 w2 = 999.00000
tsA3Z2a	0.3455548	84 C 0.699	p0 = 0.37372 p1 = 0.59772 p2a = 0.01099 p2b = 0.01757 w0 = 0.15349 w1 = 1.00000 w2 = 9.05634
tsA3Z2b	1	NA	p0 = 0.38034 p1 = 0.61966 p2a = 0.00000 p2b = 0.00000 w0 = 0.15229 w1 = 1.00000 w2 = 1.00000
tsA3Z2d	1	NA	p0 = 0.38034 p1 = 0.61966 p2a = 0.00000 p2b = 0.00000 w0 = 0.15228 w1 = 1.00000 w2 = 1.00000
tsA3Z2e	0.0544563	56 F 0.964*	p0 = 0.36611 p1 = 0.60847 p2a = 0.00955 p2b = 0.01587 w0 = 0.14754 w1 = 1.00000 w2 = 12.46350
tsA3Z2c	0.0829304	76 E 0.814, 97 L 0.529, 117 C 0.972*	p0 = 0.36194 p1 = 0.60254 p2a = 0.01333 p2b = 0.02219 w0 = 0.14623 w1 = 1.00000 w2 = 12.62593
tsA3Z2	0.0001978	26 P 0.927, 29 S 0.880, 43 K 0.847, 76 E 0.986*, 90 C 0.919 91 G 0.779	p0 = 0.35511 p1 = 0.59445 p2a = 0.01886 p2b = 0.03158 w0 = 0.15015 w1 = 1.00000 w2 = 5.77510
tsA3Z3	0.9984042	NA	p0 = 0.50257 p1 = 0.49743 p2a = 0.00000 p2b = 0.00000 w0 = 0.11457 w1 = 1.00000 w2 = 1.00000

The alignments for *APOBEC1, A3Z1, A3Z2* and *A3Z3* genes were analyzed separately for the whole sequence set. The results of positive selection analysis showed that 89H of tsAPOBEC3G (tsA3Z2c) is the positively selected site. The positive selected sites with posterior probabilities > 0.95 are marked by *.

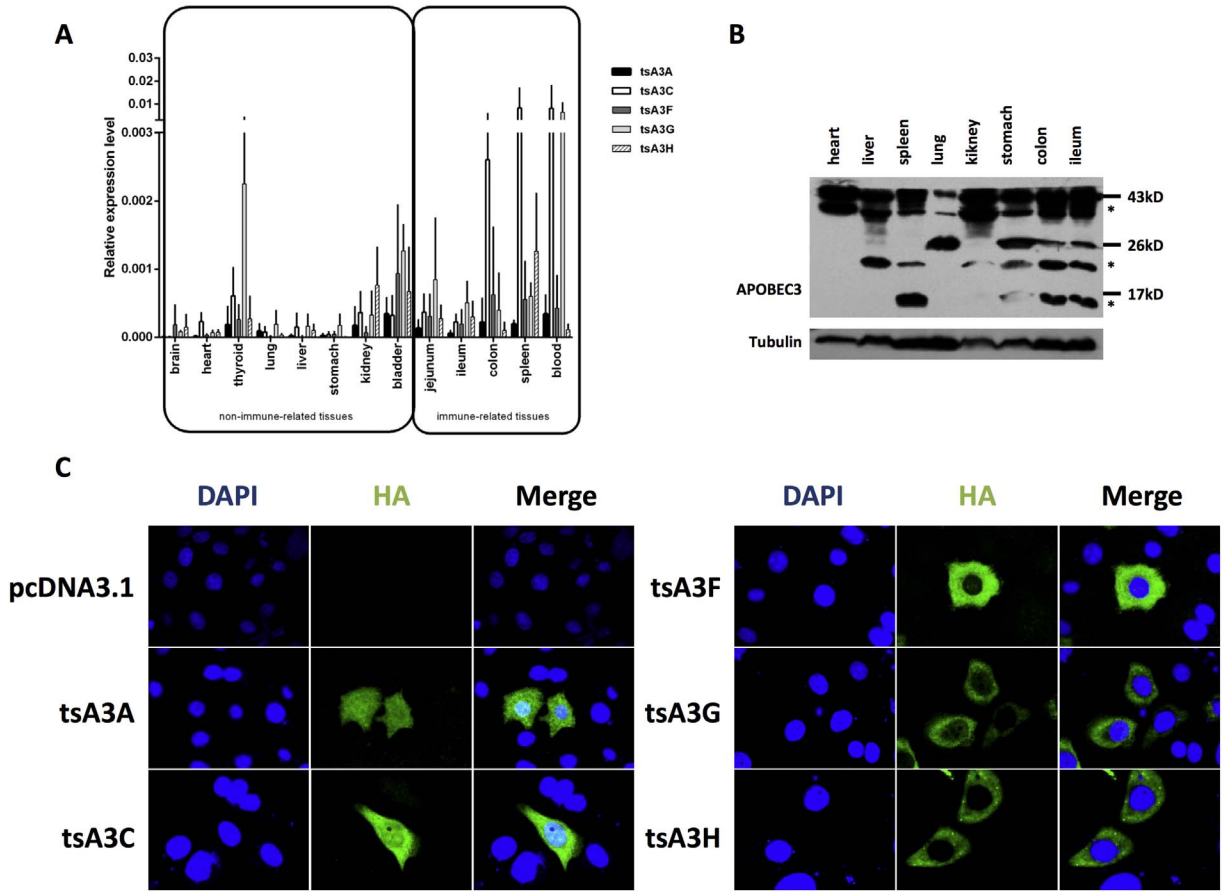

Fig. 4. tsAPOBEC3 expression patterns in different tree shrew tissues. (A) The amounts of *tsAPOBEC3* transcripts were measured by real-time quantitative PCR with specific primers, and relative gene expression was normalized to *RPL13A* within each sample. Values are the mean ± SD, The primers are shown in Table S2. The *tsAPOBEC3* mRNA had high expression in immune-related tissues, especially in the spleen. (B) Western blot for tsAPOBEC3 proteins in different tissues with monoclonal anti-hAPOBEC3G mouse antibody. The bands, marked by an asterisk, with 15 KDa, 25 KDa and 40 KDa sizes, are supposed to be tsAPOBEC3A; tsAPOBEC3H; and tsAPOBEC3C, -3F, and -3G, respectively. (C) Localization of tsAPOBEC3 in HepG2 cells by immunofluorescence staining.

response to limit viral replication. Benefitting from a high-quality genome sequence and annotation (Fan et al., 2013), CD4 (Tian et al., 2012), MHC class I (Zhang et al., 2013), CXC chemokine (Chen et al., 2014), TRIMCyp (Mu et al., 2014) and MAVS (Xu et al., 2015) were recently identified in tree shrews, showing that the tree shrew is becoming a reference in research. However, there are still many questions about the *APOBEC3* homologs in tree shrews with respect to immune factors and pathogens. In this study, we characterized the *APOBEC3* homologs in Chinese tree shrews and identified five *APOBEC3* members. These tsAPOBEC3s had high structural similarity to mammalian APOBEC3s. Furthermore, the *tsAPOBEC3 genes* followed phylogenetic patterns. However, the *tsAPOBEC3 genes* also exhibited some distinct characteristics.

The *APOBEC3 genes* have already been characterized in several species, including primates (Etienne et al., 2015), horse (Bogerd et al., 2008), pig (Dorrschuck et al., 2011), mouse (Nair et al., 2014) and cat (Munk et al., 2008). All these studies showed the diversity in the quantity and conservation of APOBEC3 active-motifs. Among newly described sequences, tsAPOBEC3 proteins shared the editing motif with human and other mammalian APOBEC3 proteins, though the number of tsAPOBEC3 was different. *tsAPOBEC3 genes* had evolved independently and underwent a strong positive selection in A3Z2. This is parallel to other mammalian APOBEC3 proteins. The genome of the mammalian ancestor encoded at least one ancestral *APOBEC3* gene, and the genome

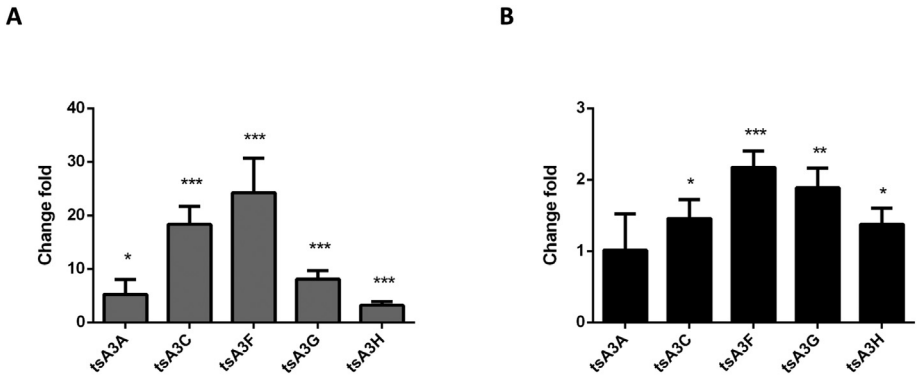

Fig. 5. Relative mRNA expression of tsAPOBEC3 in response to IFN-α2β in PBMCs and primary liver cells. (A) Primary tree shrew hepatocytes or (B) PBMCs were stimulated by 1000 U/ml IFN-α2β. Samples were taken at the start of culturing (time point 0 h) and after 12 h of culture. Total RNA was isolated and reverse transcribed, and the relative mRNA induction was determined by quantitative PCR using *RPL13A* mRNA for normalization.

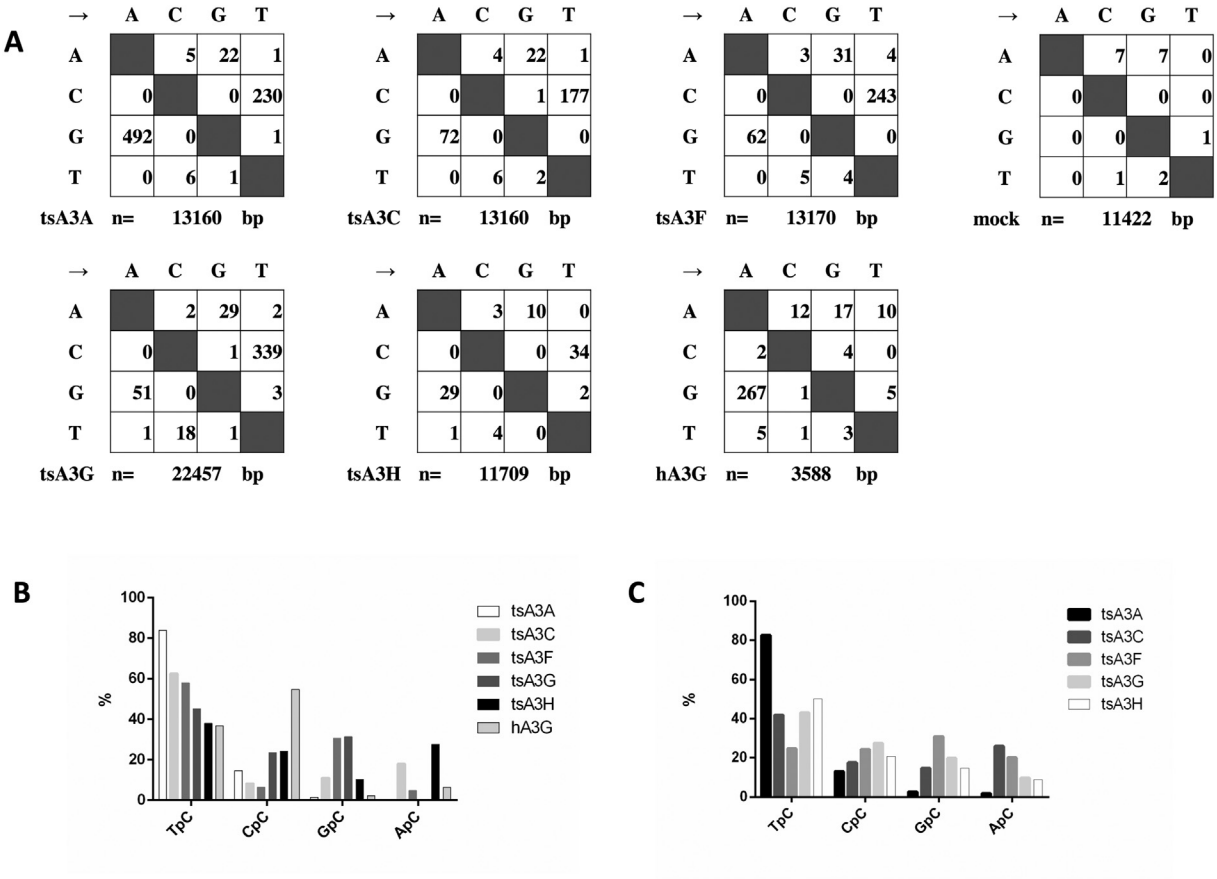

Fig. 6. Hypermutation of viral DNA in vitro by tree shrew APOBEC3 proteins. (A) The hypermutation of HIV-1 DNA by tsAPOBEC3 deamination activities were sequenced and calculated using the HIV HYPERMUT program (see before). The numbers below the boxes indicate the number of bases sequenced. (B) The 5′-dinucleotide context editing reference analysis for the G → A hypermutation in the minus strand using the HIV HYPERMUT program. (C) The 5′-dinucleotide context editing reference analysis for the C → T hypermutation in the plus strand using the HIV HYPERMUT program.

encoded an *A3Z1-A3Z2-A3Z3* arrangement between *CBX6* and *CBX7*. *APOBEC3* gene duplication events (fixation, gene loss and gene fusion) have occurred independently in different lineages (LaRue et al., 2009; Munk et al., 2012). The results of these events have led to a parallel evolution. *tsAPOBEC3 genes* evolved according this rule. Based on our results, two tsA3Z1 and five tsA3Z2 motifs diverged nearly 32.2 million years ago (Fig. 3C). This is later than tree shrew speciation, which occurred nearly 80 million years ago (Novacek, 1992), or the divergence between tree shrews and primates nearly 90.9 million years ago (Fan et al., 2013). This result supports the argument that *APOBEC3* family members from tree shrews evolved independently and demonstrates why their antiviral activities are possibly different. The function of tsAPOBEC3, which evolved independently, should be further studied.

Abnormal expression patterns often suggest that a protein has different functions. However, our results showed that *tsAPOBEC3* mRNAs and tsAPOBEC3 proteins were highly expressed in the spleen and localized in the nucleus and cytoplasm. This suggests that *tsAPOBEC3 genes* have similar expression patterns as hAPOBEC3 (Koning et al., 2009). *APOBEC3 genes* have been described as an ISG because they are activated by IFN-α stimulation (Mohanram et al., 2013). In our results, *tsAPOBEC3 genes* could be strongly stimulated by IFN-α in hepatocytes and slightly in PBMCs. These results were consistent with previous results in human cells (Tanaka et al., 2006; Wang et al., 2008). This reveals that *tsAPOBEC3 genes* also appear to be ISGs. Additionally, the editing of HBV in tree shrew hepatocytes closely overlapped that of HBV in humans (Renard et al., 2010). This suggests that not only the organization of the *tsAPOBEC3* locus and its expression pattern but also its function might resemble that of humans. However, whether tsAPOBEC3 really edits nucleic acid requires further study.

APOBEC3 proteins act as restriction factors that inhibit retroviral replication and retrotransposition by editing the DNAs of these elements (Kitamura et al., 2013; Koyama et al., 2013; Zheng et al., 2012). A comparison can be made based on the HIV-1 editing data from tsAPOBEC3s and hAPOBEC3G. The HIV-1 editing function observed for tsAPOBEC3s overlaps with the same function in humans; however, the editing of HIV-1 by tsAPOBEC3s is more likely to promote the C → T mutation than in humans. The differences between human and tree shrew editing data are striking, though the differences probably lie in the fact that the tree shrew is a natural HIV-1 host. Previous studies have documented that mouse and feline APOBEC3 had the ability of restricting HIV-1 replication and could promote G → A mutations in HIV-1 genomes (Munk et al., 2007; Nair et al., 2014). However, C → T mutations were rare in these editing events. In contrast, mouse APOBEC1 could edit the DNA plus strand and insert C → T mutations (Renard et al., 2010). Thus, the editing preferences of tsAPOBEC3s resemble that of mouse APOBEC1. This suggests that tsAPOBEC3s have distinct abilities in defense immune functions.

As an experimental animal, tree shrews have been used to study various virus infections. However, in HBV studies, only low efficiency infections have been established in tree shrews, and most infected tree shrews have spontaneously eliminated viruses within a short time (Sanada et al., 2016; Walter et al., 1996). The reasons for this are unknown. Tree shrews are generally studied due to the lack of pure inbred animals, limited access to animal resources and short references. Providing more information about innate immune restriction factors in tree shrews is another issue that needs to be urgently addressed. The tree shrew APOBEC3s, a restriction factor, should not be overlooked in innate immunity. Therefore, the functions of tsAPOBEC3s need to be

further investigated.

In summary, we characterized the *APOBEC3 genes* in tree shrews and confirmed the conservation of tsAPOBEC3 structure and function in tree shrews. This research on tsAPOBEC3s allows us to better understand innate immune responses in tree shrews. Future research will focus on deepening the antiviral functions of these editing enzymes in tree shrews. It will provide more information about innate immune restriction factors in tree shrews and be an essential guide for promoting the use of the tree shrew as a virus infection model.

Accession numbers

All the sequences reported in this paper have been deposited in GenBank (Accession numbers KU053484, KU053485, KU053486, KU053487 and KU053488).

Acknowledgements

This work was supported by grant from the 13th Five-Year Key Scientific and Technological Program of China (2017ZX10304402-002-004), National Major Program Project Grant (2016YFC1201000), the 863 Program of China (2012AA021801), the Knowledge Innovation Program of the Chinese Academy of Sciences (KSCX2-EW-J-23, KSCX2-EW-R-12), and the National Natural Science Foundation of China (U1402224).

References

Bishop, K.N., Verma, M., Kim, E.Y., Wolinsky, S.M., Malim, M.H., 2008. APOBEC3G inhibits elongation of HIV-1 reverse transcripts. PLoS Pathog. 4, e1000231. http://dx.doi.org/10.1371/journal.ppat.1000231.

Bogerd, H.P., Tallmadge, R.L., Oaks, J.L., Carpenter, S., Cullen, B.R., 2008. Equine infectious anemia virus resists the antiretroviral activity of equine APOBEC3 proteins through a packaging-independent mechanism. J. Virol. 82, 11889–11901. http://dx.doi.org/10.1128/JVI.01537-08.

Cao, J., Yang, E.B., Su, J.J., Li, Y., Chow, P., 2003. The tree shrews: adjuncts and alternatives to primates as models for biomedical research. J. Med. Primatol. 32, 123–130.

Chen, J., MacCarthy, T., 2017. The preferred nucleotide contexts of the AID/APOBEC cytidine deaminases have differential effects when mutating retrotransposon and virus sequences compared to host genes. PLoS Comput. Biol. 13 (3), e1005471. http://dx.doi.org/10.1371/journal.pcbi.1005471.

Chen, G., Wang, W., Meng, S., Zhang, L., Wang, W., Jiang, Z., et al., 2014. CXC chemokine CXCL12 and its receptor CXCR4 in tree shrews (*Tupaia belangeri*): structure, expression and function. PLoS One 9, e98231.

Dang, Y., Siew, L.M., Wang, X., Han, Y., Lampen, R., Zheng, Y.H., 2008. Human cytidine deaminase APOBEC3H restricts HIV-1 replication. J. Biol. Chem. 283, 11606–11614. http://dx.doi.org/10.1074/jbc.M707586200.

Darai, G., Schwaier, A., Komitowski, D., Munk, K., 1978. Experimental infection of *Tupaia belangeri* (tree shrews) with herpes simplex virus types 1 and 2. J. Infect. Dis. 137, 221–226.

Dorrschuck, E., Fischer, N., Bravo, I.G., Hanschmann, K.M., Kuiper, H., Spotter, A., Moller, R., Cichutek, K., Munk, C., Tonjes, R.R., 2011. Restriction of porcine endogenous retrovirus by porcine APOBEC3 cytidine deaminases. J. Virol. 85, 3842–3857. http://dx.doi.org/10.1128/JVI.01880-10.

Etienne, L., Bibollet-Ruche, F., Sudmant, P.H., Wu, L.I., Hahn, B.H., Emerman, M., 2015. The role of the antiviral APOBEC3 gene family in protecting chimpanzees against lentiviruses from monkeys. PLoS Pathog. 11, e1005149. http://dx.doi.org/10.1371/journal.ppat.1005149.

Fan, Y., Huang, Z.Y., Cao, C.C., Chen, C.S., Chen, Y.X., Fan, D.D., He, J., Hou, H.L., Hu, L., Hu, X.T., Jiang, X.T., Lai, R., Lang, Y.S., Liang, B., Liao, S.G., Mu, D., Ma, Y.Y., Niu, Y.Y., Sun, X.Q., Xia, J.Q., Xiao, J., Xiong, Z.Q., Xu, L., Yang, L., Zhang, Y., Zhao, W., Zhao, X.D., Zheng, Y.T., Zhou, J.M., Zhu, Y.B., Zhang, G.J., Wang, J., Yao, Y.G., 2013. Genome of the Chinese tree shrew. Nat. Commun. 4, 1426. http://dx.doi.org/10.1038/ncomms2416.

Fan, Y., Yu, D., Yao, Y.G., 2014. Tree shrew database (TreeshrewDB): a genomic knowledge base for the Chinese tree shrew. Sci. Rep. 4, 7145. http://dx.doi.org/10.1038/srep07145.

Fuchs, E., 2005. Social stress in tree shrews as an animal model of depression: an example of a behavioral model of a CNS disorder. CNS Spectr. 10, 182–190. http://dx.doi.org/10.1017/S1092852900010038.

Henry, M., Guetard, D., Suspene, R., Rusniok, C., Wain-Hobson, S., Vartanian, J.P., 2009. Genetic editing of HBV DNA by monodomain human APOBEC3 cytidine deaminases and the recombinant nature of APOBEC3G. PLoS One 4, e4277. http://dx.doi.org/10.1371/journal.pone.0004277.

Janahi, E.M., McGarvey, M.J., 2013. The inhibition of hepatitis B virus by APOBEC cytidine deaminases. J. Viral Hepat. 20, 821–828. http://dx.doi.org/10.1111/jvh.12192.

Jiang, L.P., Shen, Q.S., Yang, C.P., Chen, Y.B., 2017. Establishment of basal cell carcinoma animal model in Chinese tree shrew (*Tupaia belangeri* chinensis). Zool. Res. 38, 180–190. http://dx.doi.org/10.24272/j.issn.2095-8137.2017.045.

Kayesh, M.E.H., Ezzikouri, S., Chi, H., Sanada, T., Yamamoto, N., Kitab, B., Haraguchi, T., Matsuyama, R., Nkogue, C.N., Hatai, H., Miyoshi, N., Murakami, S., Tanaka, Y., Takano, J.I., Shiogama, Y., Yasutomi, Y., Kohara, M., Tsukiyama-Kohara, K., 2017. Interferon-beta response is impaired by hepatitis B virus infection in *Tupaia belangeri*. Virus Res. 237, 47–57. http://dx.doi.org/10.1016/j.virusres.2017.05.013.

Kayesh, M.E.H., Kitab, B., Sanada, T., Hayasaka, D., Morita, K., Kohara, M., Tsukiyama-Kohara, K., 2017. Susceptibility and initial immune response of *Tupaia belangeri* cells to dengue virus infection. Infect. Genet. Evol. 51, 203–210. http://dx.doi.org/10.1016/j.meegid.2017.04.003.

Kitamura, K., Wang, Z., Chowdhury, S., Simadu, M., Koura, M., Muramatsu, M., 2013. Uracil DNA glycosylase counteracts APOBEC3G-induced hypermutation of hepatitis B viral genomes: excision repair of covalently closed circular DNA. PLoS Pathog. 9, e1003361. http://dx.doi.org/10.1371/journal.ppat.1003361.

Kock, J., Baumert, T.F., Delaney, W.E.T., Blum, H.E., von Weizsacker, F., 2003. Inhibitory effect of adefovir and lamivudine on the initiation of hepatitis B virus infection in primary tupaia hepatocytes. Hepatology 38, 1410–1418. http://dx.doi.org/10.1016/j.hep.2003.09.009.

Koning, F.A., Newman, E.N., Kim, E.Y., Kunstman, K.J., Wolinsky, S.M., Malim, M.H., 2009. Defining APOBEC3 expression patterns in human tissues and hematopoietic cell subsets. J. Virol. 83, 9474–9485. http://dx.doi.org/10.1128/JVI.01089-09.

Koyama, T., Arias, J.F., Iwabu, Y., Yokoyama, M., Fujita, H., Sato, H., Tokunaga, K., 2013. APOBEC3G oligomerization is associated with the inhibition of both Alu and LINE-1 retrotransposition. PLoS One 8, e84228. http://dx.doi.org/10.1371/journal.pone.0084228.

LaRue, R.S., Andresdottir, V., Blanchard, Y., Conticello, S.G., Derse, D., Emerman, M., Greene, W.C., Jonsson, S.R., Landau, N.R., Lochelt, M., Malik, H.S., Malim, M.H., Munk, C., O'Brien, S.J., Pathak, V.K., Strebel, K., Wain-Hobson, S., Yu, X.F., Yuhki, N., Harris, R.S., 2009. Guidelines for naming nonprimate APOBEC3 genes and proteins. J. Virol. 83, 494–497. http://dx.doi.org/10.1128/JVI.01976-08.

Li, S.A., Lee, W.H., Zhang, Y., 2012. Two bacterial infection models in tree shrew for evaluating the efficacy of antimicrobial agents. Zool. Res. 33 (1), 1–6. http://dx.doi.org/10.3724/SP.J.1141.2012.01001.

Li, L.H., Li, Z.R., Wang, E.L., Yang, R., Xiao, Y., Han, H.B., Lang, F.C., Li, X., Xia, Y.J., Gao, F., Li, Q.H., Fraser, N.W., Zhou, J.M., 2016. Herpes simplex virus 1 infection of tree shrews differs from that of mice in the severity of acute infection and viral transcription in the peripheral nervous system. J. Virol. 90, 790–804. http://dx.doi.org/10.1128/JVI.02258-15.

Li, J.P., Liao, Y., Zhang, Y., Wang, J.J., Wang, L.C., Feng, K., Li, Q.H., Liu, L.D., 2014. Experimental infection of tree shrews (*Tupaia belangeri*) with Coxsackie virus A16. Zool. Res. 35, 485–491. http://dx.doi.org/10.13918/j.issn.2095-8137.2014.6.485.

Mohanram, V., Skold, A.E., Bachle, S.M., Pathak, S.K., Spetz, A.L., 2013. IFN-alpha induces APOBEC3G, F, and A in immature dendritic cells and limits HIV-1 spread to CD4 + T cells. J. Immunol. 190, 3346–3353. http://dx.doi.org/10.4049/jimmunol.1201184.

Mu, D., Yang, H., Zhu, J.W., Liu, F.L., Tian, R.R., Zheng, H.Y., Han, J.B., Shi, P., Zheng, Y.T., 2014. Independent birth of a novel TRIMCyp in *Tupaia belangeri* with a divergent function from its paralog TRIM5. Mol. Biol. Evol. 31, 2985–2997. http://dx.doi.org/10.1093/molbev/msu238.

Munk, C., Beck, T., Zielonka, J., Hotz-Wagenblatt, A., Chareza, S., Battenberg, M., Thielebein, J., Cichutek, K., Bravo, I.G., O'Brien, S.J., Lochelt, M., Yuhki, N., 2008. Functions, structure, and read-through alternative splicing of feline APOBEC3 genes. Genome Biol. 9, R48. http://dx.doi.org/10.1186/gb-2008-9-3-r48.

Munk, C., Willemsen, A., Bravo, I.G., 2012. An ancient history of gene duplications, fusions and losses in the evolution of APOBEC3 mutators in mammals. BMC Evol. Biol. 12, 71. http://dx.doi.org/10.1186/1471-2148-12-71.

Munk, C., Zielonka, J., Constabel, H., Kloke, B.P., Rengstl, B., Battenberg, M., Bonci, F., Pistello, M., Lochelt, M., Cichutek, K., 2007. Multiple restrictions of human immunodeficiency virus type 1 in feline cells. J. Virol. 81, 7048–7060. http://dx.doi.org/10.1128/JVI.02714-06.

Nair, S., Sanchez-Martinez, S., Ji, X., Rein, A., 2014. Biochemical and biological studies of mouse APOBEC3. J. Virol. 88, 3850–3860. http://dx.doi.org/10.1128/JVI.03456-13.

Nakaya, Y., Stavrou, S., Blouch, K., Tattersall, P., Ross, S.R., 2016. *In vivo* examination of mouse APOBEC3- and human APOBEC3A- and APOBEC3G- mediated restriction of parvovirus and herpesvirus infection in mouse models. J. Virol. 90, 8005–8012. http://dx.doi.org/10.1128/JVI.00973-16.

Nguyen, D.H., Gummuluru, S., Hu, J., 2007. Deamination-independent inhibition of hepatitis B virus reverse transcription by APOBEC3G. J. Virol. 81, 4465–4472. http://dx.doi.org/10.1128/JVI.02510-06.

Novacek, M.J., 1992. Mammalian phylogeny: shaking the tree. Nature 356, 121–125. http://dx.doi.org/10.1038/356121a0.

Nowarski, R., Prabhu, P., Kenig, E., Smith, Y., Britan-Rosich, E., Kotler, M., 2014. APOBEC3G inhibits HIV-1 RNA elongation by inactivating the viral trans-activation response element. J. Mol. Biol. 426, 2840–2853. http://dx.doi.org/10.1016/j.jmb.2014.05.012.

Petit, V., Guetard, D., Renard, M., Keriel, A., Sitbon, M., Wain-Hobson, S., Vartanian, J.P., 2009. Murine APOBEC1 is a powerful mutator of retroviral and cellular RNA *in vitro* and *in vivo*. J. Mol. Biol. 385, 65–78. http://dx.doi.org/10.1016/j.jmb.2008.10.043.

Renard, M., Henry, M., Guetard, D., Vartanian, J.P., Wain-Hobson, S., 2010. APOBEC1 and APOBEC3 cytidine deaminases as restriction factors for hepadnaviral genomes in non-humans *in vivo*. J. Mol. Biol. 400, 323–334. http://dx.doi.org/10.1016/j.jmb.2010.05.029.

Roberts, T.E., Lanier, H.C., Sargis, E.J., Olson, L.E., 2011. Molecular phylogeny of treeshrews (Mammalia: *Scandentia*) and the timescale of diversification in Southeast

Asia. Mol. Phylogenet. Evol. 60, 358–372. http://dx.doi.org/10.1016/j.ympev.2011.04.021.

Rogozin, I.B., Basu, M.K., Jordan, I.K., Pavlov, Y.I., Koonin, E.V., 2005. APOBEC4, a new member of the AID/APOBEC family of polynucleotide (deoxy)cytidine deaminases predicted by computational analysis. Cell Cycle 4, 1281–1285. http://dx.doi.org/10.4161/cc.4.9.1994.

Sakurai, D., Iwatani, Y., Ohtani, H., Naruse, T.K., Terunuma, H., Sugiura, W., Kimura, A., 2015. APOBEC3H polymorphisms associated with the susceptibility to HIV-1 infection and AIDS progression in Japanese. Immunogenetics 67, 253–257. http://dx.doi.org/10.1007/s00251-015-0829-2.

Sanada, T., Tsukiyama-Kohara, K., Yamamoto, N., Ezzikouri, S., Benjelloun, S., Murakami, S., Tanaka, Y., Tateno, C., Kohara, M., 2016. Property of hepatitis B virus replication in *Tupaia belangeri* hepatocytes. Biochem. Biophys. Res. Commun. 469, 229–235. http://dx.doi.org/10.1016/j.bbrc.2015.11.121.

Seppen, J., 2004. Unedited inhibition of HBV replication by APOBEC3G. J. Hepatol. 41, 1068–1069. http://dx.doi.org/10.1016/j.jhep.2004.10.008.

Stamatakis, A., 2014. RAxML version 8: a tool for phylogenetic analysis and post-analysis of large phylogenies. Bioinformatics 30, 1312–1313. http://dx.doi.org/10.1093/bioinformatics/btu033.

Stavrou, S., Blouch, K., Kotla, S., Bass, A., Ross, S.R., 2015. Nucleic acid recognition orchestrates the anti-viral response to retroviruses. Cell Host Microbe 17, 478–488. http://dx.doi.org/10.1016/j.chom.2015.02.021.

Tanaka, Y., Marusawa, H., Seno, H., Matsumoto, Y., Ueda, Y., Kodama, Y., Endo, Y., Yamauchi, J., Matsumoto, T., Takaori-Kondo, A., Ikai, I., Chiba, T., 2006. Anti-viral protein APOBEC3G is induced by interferon-alpha stimulation in human hepatocytes. Biochem. Biophys. Res. Commun. 341, 314–319. http://dx.doi.org/10.1016/j.bbrc.2005.12.192.

Tian, W.W., Gao, Y.D., Guo, Y., Huang, J.F., Xiao, C., Li, Z.S., et al., 2012. Cloning of full-length coding sequence of tree shrew CD4 and prediction of its molecular characteristics. Zool. Res. 33, 60–66. http://dx.doi.org/10.3724/SP.J.1141.2012.01060.

Vieira, V.C., Soares, M.A., 2013. The role of cytidine deaminases on innate immune responses against human viral infections. Biomed. Res. Int. 2013, 683095. http://dx.doi.org/10.1155/2013/683095.

Walter, E., Keist, R., Niederost, B., Pult, I., Blum, H.E., 1996. Hepatitis B virus infection of tupaia hepatocytes *in vitro* and *in vivo*. Hepatology 24, 1–5. http://dx.doi.org/10.1002/hep.510240101.

Wang, F.X., Huang, J.L., Zhang, H.X., Ma, X.L., Zhang, H., 2008. APOBEC3G upregulation by alpha interferon restricts human immunodeficiency virus type 1 infection in human peripheral plasmacytoid dendritic cells. J. Gen. Virol. 89, 722–730. http://dx.doi.org/10.1099/vir.0.83530-0.

Wang, Z., Wakae, K., Kitamura, K., Aoyama, S., Liu, G.Y., Koura, M., Monjurul, A.M., Kukimoto, I., Muramatsu, M., 2014. APOBEC3 deaminases induce hypermutation in human papillomavirus 16 DNA upon beta interferon stimulation. J. Virol. 88, 1308–1317. http://dx.doi.org/10.1128/JVI.03091-13.

Wei, S., Hua, H.R., Chen, Q.Q., Zhang, Y., Chen, F., Li, S.Q., et al., 2017. Dynamic changes in DNA demethylation in the tree shrew (*Tupaia belangeri* chinensis) brain during postnatal development and aging. Zool. Res. 38, 96–102. http://dx.doi.org/10.24272/j.issn.2095-8137.2017.013.

Xiao, J., Liu, R., Chen, C.S., 2017. Tree shrew (*Tupaia belangeri*) as a novel laboratory disease animal model. Zool. Res. 38 (3), 127–137. http://dx.doi.org/10.24272/j.issn.2095-8137.2017.033.

Xu, L., Yu, D., Peng, L., Fan, Y., Chen, J., Zheng, Y.T., Wang, C., Yao, Y.G., 2015. Characterization of a MAVS ortholog from the Chinese tree shrew (*Tupaia belangeri* chinensis). Dev. Comp. Immunol. 52, 58–68. http://dx.doi.org/10.1016/j.dci.2015.04.014.

Xu, L., Zhang, Y., Liang, B., Lu, L.B., Chen, C.S., Chen, Y.B., Zhou, J.M., Yao, Y.G., 2013. Tree shrews under the spot light: emerging model of human diseases. Zool. Res. 34, 59–69. http://dx.doi.org/10.3724/SP.J.1141.2013.02059.

Yan, L.Z., Sun, B., Lyu, L.B., Ma, Y.H., Chen, J.Q., Lin, Q., et al., 2016. Early embryonic development and transplantation in tree shrews. Zool. Res. 37, 252–258. http://dx.doi.org/10.13918/j.issn.2095-8137.2016.4.252.

Yang, Z., 2007. PAML 4: phylogenetic analysis by maximum likelihood. Mol. Biol. Evol. 24, 1586–1591. http://dx.doi.org/10.1093/molbev/msm088.

Yang, Z.F., Zhao, J., Zhu, Y.T., Wang, Y.T., Liu, R., Zhao, S.S., Li, R.F., Yang, C.G., Li, J.Q., Zhong, N.S., 2013. The tree shrew provides a useful alternative model for the study of influenza H1N1 virus. Virol. J. 10, 111. http://dx.doi.org/10.1186/1743-422X-10-111.

Yao, Y.G., 2017. Creating animal models, why not use the Chinese tree shrew (*Tupaia belangeri* chinensis). Zool. Res. 38 (3), 118–126. http://dx.doi.org/10.24272/j.issn.2095-8137.2017.032.

Zhang, X.H., Dai, Z.X., Zhang, G.H., Han, J.B., Zheng, Y.T., 2013. Molecular characterization, balancing selection, and genomic organization of the tree shrew (*Tupaia belangeri*) MHC class I gene. Gene 522, 147–155. http://dx.doi.org/10.1016/j.gene.2013.03.113.

Zhao, X.P., Tang, Z.Y., Klumpp, B., Wolff-Vorbeck, G., Barth, H., Levy, S., von Weizsacker, F., Blum, H.E., Baumert, T.F., 2002. Primary hepatocytes of *Tupaia belangeri* as a potential model for hepatitis C virus infection. J. Clin. Invest. 109, 221–232. http://dx.doi.org/10.1172/JCI13011.

Zheng, Y.H., Jeang, K.T., Tokunaga, K., 2012. Host restriction factors in retroviral infection: promises in virus-host interaction. Retrovirology 9, 112. http://dx.doi.org/10.1186/1742-4690-9-112.

Zheng, Y.T., Yao, Y.G., Xu, L., 2014. Basic Biology and Disease Models of Tree Shrews. Yunnan Science and Technology Press, Kunming.